ORIGINAL RESEARCH

An Integrated Systems Biology Approach Identifies the Proteasome as A Critical Host Machinery for ZIKV and DENV Replication

Guang Song [1,#], Emily M. Lee [2,#], Jianbo Pan [3,#], Miao Xu [4,5,#], Hee-Sool Rho [1], Yichen Cheng [2], Nadia Whitt [4], Shu Yang [4], Jennifer Kouznetsova [4], Carleen Klumpp-Thomas [4], Samuel G. Michael [4], Cedric Moore [1], Ki-Jun Yoon [6,7], Kimberly M. Christian [7], Anton Simeonov [4], Wenwei Huang [4], Menghang Xia [4], Ruili Huang [4], Madhu Lal-Nag [4,*], Hengli Tang [2,*], Wei Zheng [4,*], Jiang Qian [3,*], Hongjun Song [6,7,8,9,10,*], Guo-li Ming [6,7,8,9,*], Heng Zhu [1,*]

[1] Department of Pharmacology & Molecular Sciences, Johns Hopkins School of Medicine, Baltimore, MD 21205, USA
[2] Department of Biological Science, Florida State University, Tallahassee, FL 32306, USA
[3] Department of Ophthalmology, Johns Hopkins School of Medicine, Baltimore, MD 21205, USA
[4] National Center for Advancing Translational Sciences, National Institutes of Health, Bethesda, MD 20892, USA
[5] Sir Run Run Shaw Hospital, Zhejiang University School of Medicine, Hangzhou 310016, China
[6] Institute for Cell Engineering, Johns Hopkins University School of Medicine, Baltimore, MD 21205, USA
[7] Department of Neuroscience and Mahoney Institute for Neurosciences, Perelman School for Medicine, University of Pennsylvania, Philadelphia, PA 19104, USA
[8] Department of Cell and Developmental Biology, Perelman School for Medicine, University of Pennsylvania, Philadelphia, PA 19104, USA
[9] Institute for Regenerative Medicine, Perelman School for Medicine, University of Pennsylvania, Philadelphia, PA 19104, USA
[10] The Epigenetics Institute, Perelman School for Medicine, University of Pennsylvania, Philadelphia, PA 19104, USA

* Corresponding authors.
E-mail: Madhu.Lal@nih.gov (Lal-Nag M), tang@bio.fsu.edu (Tang H), wzheng@mail.nih.gov (Zheng W), jiang.qian@jhmi.edu (Qian J), shongjun@pennmedicine.upenn.edu (Song H), gming@pennmedicine.upenn.edu (Ming Gl), hzhu4@jhmi.edu (Zhu H).
\# Equal contribution.

Abstract The Zika virus (ZIKV) and dengue virus (DENV) flaviviruses exhibit similar replicative processes but have distinct clinical outcomes. A systematic understanding of virus–host **protein–protein interaction** networks can reveal cellular pathways critical to viral replication and disease pathogenesis. Here we employed three independent systems biology approaches toward this goal. First, protein array analysis of direct interactions between individual ZIKV/DENV viral proteins and 20,240 human proteins revealed multiple conserved cellular pathways and protein complexes, including proteasome complexes. Second, an **RNAi screen** of 10,415 druggable genes identified the host proteins required for ZIKV infection and uncovered that proteasome proteins were crucial in this process. Third, high-throughput screening of 6016 bioactive compounds for ZIKV inhibition yielded 134 effective compounds, including six proteasome inhibitors that suppress both ZIKV and DENV replication. Integrative analyses of these orthogonal datasets pinpoint proteasomes as critical host machinery for ZIKV/DENV replication. Our study provides **multi-omics** datasets for further studies of flavivirus–host interactions, disease pathogenesis, and new drug targets.

Introduction

The dengue virus (DENV) and Zika virus (ZIKV) are two closely related pathogens of the Flaviviridae family [1]. Although dengue disease has been recognized in the Americas since the 1600's, DENV was only isolated in 1943 and is still one of the most widespread global mosquito-borne viruses. DENV contributes to symptoms in 96 million people and results in over 20,000 deaths each year [2,3]. ZIKV was first discovered as a mild, obscure human pathogen in 1947, but has emerged as a major public health concern in the past few years. This is largely due to its role as an etiological agent in several neurological pathologies, including congenital microcephaly and Guillain–Barre syndrome [4].

The genomes of both DENV and ZIKV are composed of a single positive-strand RNA, which is directly translated into a polyprotein and subsequently processed to generate components necessary for viral replication and assembly [1]. Because of the limited number of proteins encoded by viral genomes, these viruses are obligate intracellular pathogens. This means that they are completely dependent on their hosts for survival and reproduction, which is mediated by direct interactions between the virus and host cellular components [5–7]. A better understanding of virus–host interactions can reveal critical cellular pathways that are necessary for viral replication and pathogenesis. In turn, this could be used to identify effective treatment regimens targeting host proteins [5,7–9]. Advancements in high-throughput technologies over the last decade have made it possible to systematically analyze the protein–protein interactome between a virus and its host [10–14]. Previous studies have identified several new host pathways that are essential to the life cycles of several pathogens, including Kaposi's sarcoma-associated herpesvirus (KSHV) [15–18], influenza virus [19], HIV [20], and Epstein–Barr virus [21].

Most antiviral drugs are classified as direct-acting antivirals (DAAs). DAAs directly target specific viral proteins critical for infection. While there are many successful DAAs currently in use for viral infections (*e.g.*, hepatitis C virus), it is well-known that many RNA viruses rapidly develop drug resistance. This is due to the selective stress imparted by targeting essential viral proteins and the high mutation rate in their RNA-based genomes [22,23]. For this reason, a drug targeting

critical host proteins would provide a higher genetic barrier for a virus to develop drug resistance [6].

Genetic similarities between DENV and ZIKV, together with recent findings about the host cell dependency factors they share, suggest that these two related flaviviruses likely utilize a similar replicative strategy in the host [24,25]. Consequently, characterization of conserved flavivirus–human protein–protein interactions (PPIs) can reveal critical cellular pathways that are essential for flavivirus infection [5,25,26]. On the other hand, differences in PPIs between ZIKV and DENV may provide insight into how these two viruses lead to different pathological outcomes, for example, microcephaly induced by ZIKV [27]. Here, we comprehensively surveyed the human proteome with individual ZIKV and DENV proteins to identify virus–host PPI networks. Bioinformatic analyses revealed multiple cellular pathways and protein complexes, including the proteasome complex. In parallel, a RNAi screen targeting druggable genes in combination with a high-throughput chemical genetics approach also revealed overlapping cellular pathways and protein complexes. Through integrative analysis of these three omics datasets, we identified several conserved cellular machineries important for ZIKV and DENV infection, including the proteasome complex. Cell-based assays confirmed that proteasome inhibitors effectively suppressed both ZIKV and DENV replication. Together, our study not only provides a valuable multi-omics dataset resource for the field, but also suggests new strategies for understanding the molecular mechanisms of virus–host interactions and pathogenesis and for identifying cellular host-based targets to develop antiviral therapeutics.

Results

ZIKV and DENV recombinant proteins

The flavivirus genome encodes a total of ten proteins, including three structural proteins and seven non-structural proteins. The three structural proteins are the capsid protein (C); the pre-membrane protein (prM), which is subsequently cleaved upon viral maturation into a Pr peptide and a mature membrane protein (M); and the envelope protein (E), which mediates fusion between viral and cellular membranes. The seven

non-structural proteins are non-structural protein 1 (NS1), which is required for formation of the replication complex and recruitment of other non-structural proteins to the ER-derived membrane structures; NS2A, which is involved in virion assembly and antagonizes the host alpha/beta interferon antiviral response; serine protease NS2B; serine protease NS3; NS4A, which regulates the ATPase activity of NS3; NS4B, which induces the formation of ER-derived membrane vesicles; RNA-directed RNA polymerase NS5; and the short peptide 2K [28]. To construct ZIKV– and DENV–host PPI networks, we cloned the genes from the ZIKV MR766 strain (African strain) and DENV serotype 1 (Figure S1A). We confirmed cloning fidelity by Sanger sequencing (Figure S1B–D; Table S1). Using a previously reported protocol [21], the viral proteins were individually purified from yeast as N-terminal tagged GST fusion proteins and fluorescently labeled (Figure S1E). The quality and quantity of these labeled proteins were evaluated using SDS-PAGE (Figure S1E).

Considering the various post-translational modifications (*e.g.*, glycosylation) catalyzed by yeast cells and the importance of correct disulfide bond formation on a protein's function and binding activity, we decided to focus on the six homologous non-structural proteins (*i.e.*, NS2A, NS2B, NS3, NS4A, NS4B, and NS5) and two variants with the signal peptide 2K (*i.e.*, NS4A + 2K and 2K + NS4B) encoded by ZIKV MR766 strain and DENV serotype 1 to construct virus–host PPI networks.

Construction of ZIKV– and DENV–human PPIs

The Human Proteome Microarray v3.0 (HuProt™ array), comprised of 20,240 immobilized human proteins from > 15,000 full-length genes, was used to identify virus–human PPI networks [29]. Each viral protein was fluorescently labeled and individually probed on the HuProt array. Fluorescent signals indicating viral protein bound to immobilized human protein were acquired, normalized, and quantified [30]. We used a very stringent cut-off (Z-score ≥ 15) to identify positive hits for each viral protein (**Figure 1**A). The assays performed in duplicate showed high reproducibility as measured by Pearson correlation coefficients. An example of binding signals obtained with DENV-NS5 is shown in Figure 1B.

We identified a total of 1708 ZIKV–host PPIs and 1408 DENV–host PPIs, involving 581 human proteins (Table S2). The majority of host proteins were found to interact with specific individual viral proteins. For example, 152 human proteins only interacted with a single viral protein, whereas 75 human proteins bound to two viral proteins (Figure S2A). We found 24 human proteins that interacted with all viral proteins tested, which is possibly a consequence of the common N-terminal GST tag. These 24 human proteins were removed from further analysis.

We recently used the NS2A PPI dataset to investigate how ZIKV-NS2A causes microcephaly-like phenotypes in the embryonic mouse cortex and human forebrain organoid models [27]. Using a co-immunoprecipitation (Co-IP) assay, we confirmed interactions between ZIKV-NS2A and three endogenous PPI targets (ARPC3, SMAD7, and NUMBL) in neural stem cells [27]. We also evaluated the ability of our approach to recover human proteins known to be targeted by viruses. We acquired a total of 754 human targets from Vir-

usMINT [31] and Virhostome [32]. Of the 557 host proteins identified in our PPI analysis, 54 overlapped with the 754 targets from VirusMINT and Virhostome (hypergeometric *P* value = 1.9E−5; Figure S2B). The result that only around 10% of the identified hits were shared with the other two databases may be due to the use of different technologies, or due to the fact that different varieties of the virus have specific binding proteins to maintain their replication. Furthermore, we noted that a recently published paper identified 701 and 688 human binding proteins by IP-MS and BioID, respectively (Figure S2C), both of which were based on MS [33]. Of these, 48 overlapped with our 581 host proteins (hypergeometric *P* value = 0.004).

Host cellular machineries involved in PPIs

To compare PPIs between ZIKV and DENV, we assembled a global PPI network involving 557 human, 8 ZIKV, and 8 DENV protein nodes (Figure S2D; Table S2). From this data, 110 and 42 host proteins were exclusively connected to a single ZIKV or DENV protein, respectively, suggesting that these virus-specific PPIs could contribute to ZIKV- or DENV-specific infection outcomes or pathological effects. For example, PLEK was connected only to ZIKV-NS2A; DDX49 and TTR only to ZIKV-NS4B; and 75 proteins only to ZIKV-NS4A. Our recent study also confirmed the interactions of ARPC3 and NUMBL to ZIKV-NS2A but not to DENV-NS2A, which was identified in our previous study by using a Co-IP method in HEK293 cells [27].

In the PPI networks, 368 (66.1%) human proteins were connected to both ZIKV and DENV homologous proteins, supporting the notion that these two related viruses exploit similar cellular machineries. Statistical analysis showed a significant overlap between human proteins recognized among each viral homologous protein pair (Figure 1C). For example, ZIKV-NS3 and DENV-NS3 proteins were found to interact with 238 and 240 human proteins, respectively, of which 187 were shared (77.9%−78.6%; hypergeometric *P* value = 3.7E−324). Conversely, ZIKV-NS3 and ZIKV-NS4A, two unrelated proteins, interacted with 238 and 401 human proteins, respectively, of which only 168 overlapped (41.9%−70.6%). Similarly, only 127 proteins (52.9%−67.6%) overlapped between 240 DENV-NS3 bound and 188 DENV-NS4A bound human proteins.

Gene Ontology (GO) analysis for human proteins that were targeted by each individual viral protein revealed several interesting GO features (**Figure 2**A; Table S3). First, host proteins connected to homologous ZIKV and DENV proteins were often enriched for the same GO terms. This is consistent with the result that a large number of shared host proteins interacted with homologous viral proteins. Second, host proteins targeted by different viral proteins were enriched for diverse biological processes and protein complexes. Third, many different viral proteins interacted with different components of the same enriched biological processes and protein complexes.

These observations raised the question of whether the conserved and virus-specific PPIs reflected different biological processes. Indeed, GO analysis of ZIKV/DENV conserved PPIs and ZIKV- or DENV-specific PPIs demonstrated distinct enrichments (Figure 2A). For instance, the GO term of cell–cell adhesion was enriched mainly in human proteins specifi-
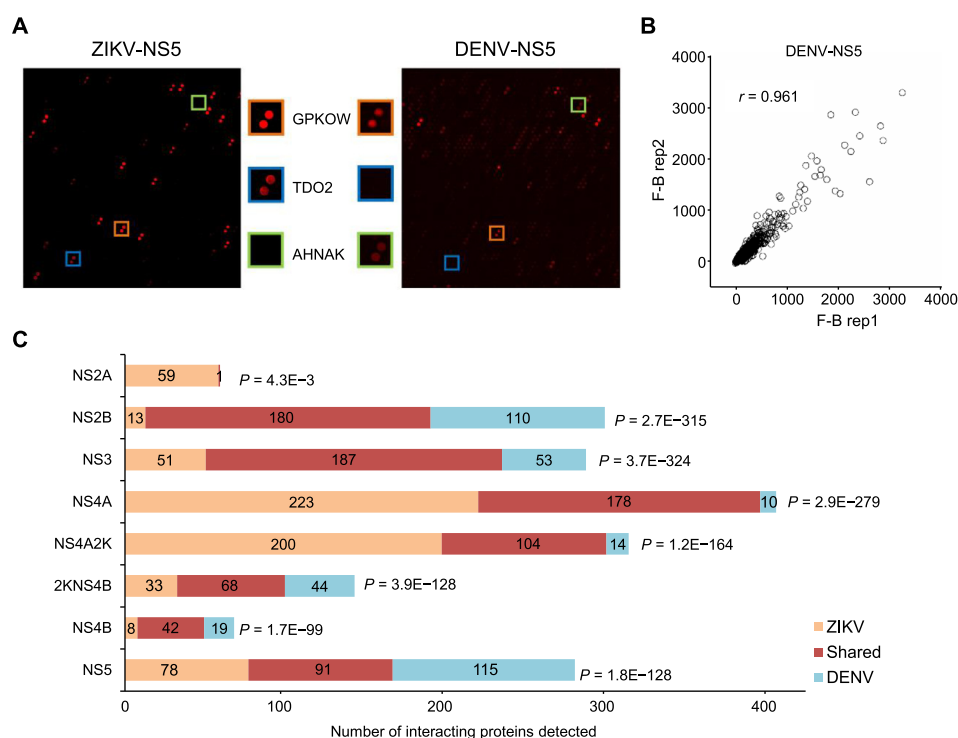
Figure 1   Identification of ZIKV– and DENV–host PPIs
A. Sample images of HuProt arrays showing human proteins bound by individual viral proteins. Each human protein was printed in duplicate. The orange, blue, and green boxes represent shared, ZIKV-specific, and DENV-specific interactions, respectively. **B.** Duplicate experiments performed for each viral protein probe showed high reproducibility. Pearson correlation coefficient analysis showed that signals of duplicate experiments based on DENV-NS5 have a high linear relationship ($r = 0.961$). **C.** Summary of numbers of unique and conserved virus–host interactions between each ZIKV and DENV homologous pair.

cally targeted by ZIKV proteins. On the other hand, GO terms of proteasome complex and NIK/NF-kappaB signaling were enriched in PPIs shared by ZIKV and DENV, suggesting that these virus-relevant protein complexes and biological processes may be important for flavivirus infections. For example, six of the non-structural ZIKV proteins (NS2B, NS3, NS4A, NS4A + 2K, 2K + NS4B, and NS5) interact with eight components in the proteasome complex (Figure 2B). Similar phenomena were observed for the spliceosome complex (Figure 2C). Furthermore, Co-IP performed in HEK293FT cells verified the physical binding of proteasome subunits PSMA3/PSMB4 to ZIKV-NS3 and PSMA1/PSMA3/PSMB4 to ZIKV-NS5 (Figure 2D). Consistent with our finding, a recent study reported that DENV-NS5 protein interfered with host mRNA splicing through direct binding to proteins in the spliceosome complex [34].

RNAi screening identified critical host proteins

To validate whether host proteins enriched in the aforementioned biological processes and protein complexes were functionally involved in ZIKV infection, we carried out a siRNA-knockdown assay similar to those used for other viruses [12,35–38]. Specifically, 10,415 druggable target genes were individually knocked down and ZIKV NS1 protein level was measured using a high-throughput homogenous time-resolved fluorescence (HTRF) assay as a surrogate for viral load in ZIKV-infected HEK293 cells. Among the 10,415 target

genes, knockdown of 120 (1.2%) genes resulted in significantly reduced NS1 levels (> 30%; Table S4). GO analysis revealed that proteasome, spliceosome, RNA polymerase, COPI vesicle coat, and Eukaryotic 43S preinitiation complex were significantly enriched among those 120 genes, with proteasome showing the lowest P value ($P = 3.8E-25$; Figure 3A).

Of the 10,415 target genes, protein products of 327 genes were found to interact with ZIKV proteins during our PPI analysis, and individual siRNA-knockdown of three of them (*i.e.*, *PSMC3*, *PSMA1*, and *OVOL2*) resulted in > 30% reduction of NS1 levels. Notably, a significant increase in the success rate of the knockdown assays was observed for those genes whose protein products were found in the enriched GO terms identified by the PPI analysis (Figure 3B). For example, individual knockdown of 20 of the 47 members (42.5%) in the proteasome complex showed > 30% reduction of NS1 levels (Figure 3B).

High-throughput drug screening identified small molecule inhibitors

To further substantiate our results, we employed an independent chemical genetics approach to screen for and validate chemical compounds that target host proteins essential for viral replication and that interfere with the ZIKV life cycle. A total of 6016 compounds, including the Library of Pharmacologically Active Compounds (LOPAC, 1280 compounds), the NIH Chemical Genomics Center (NCGC) pharmaceutical
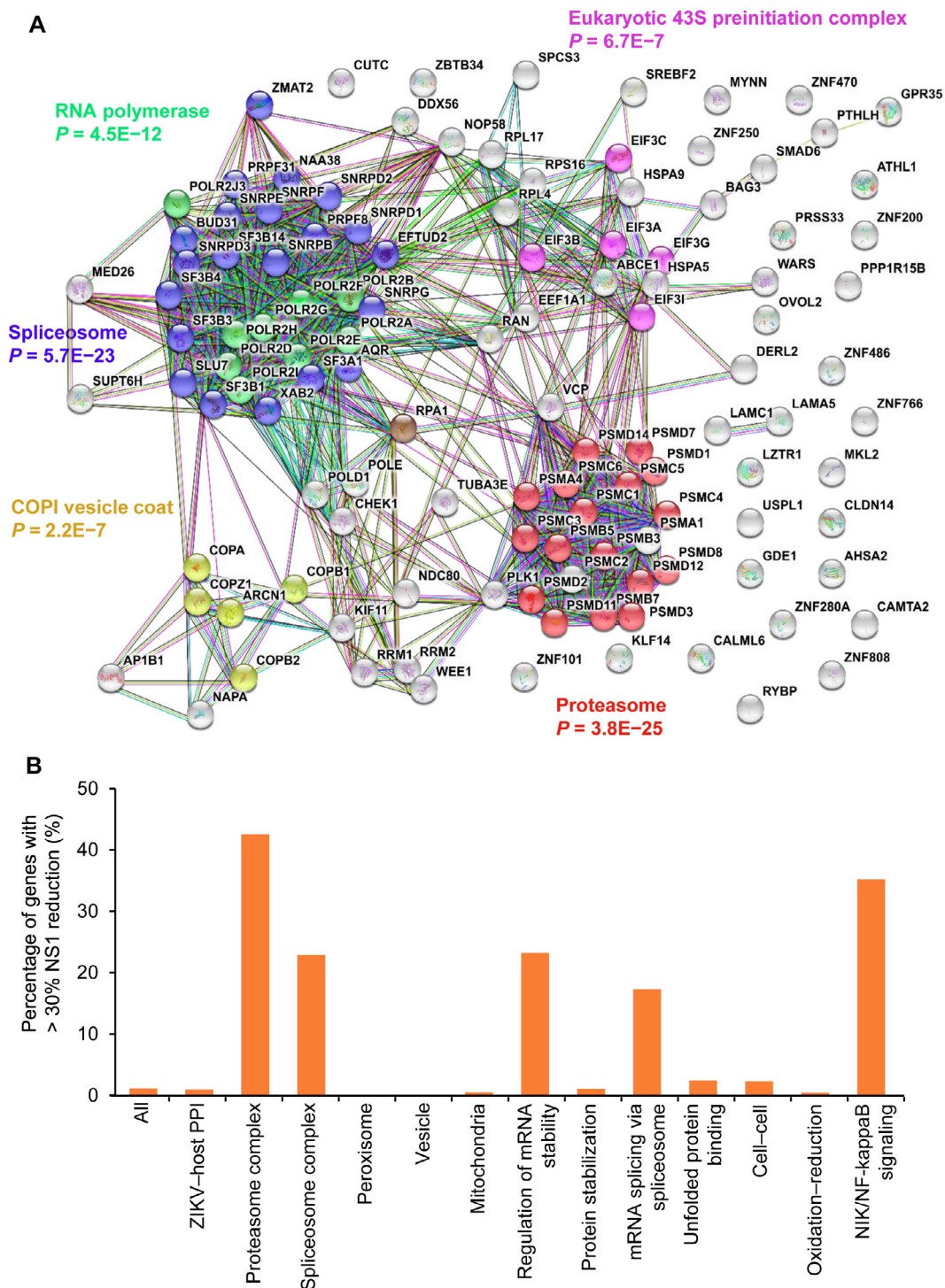
Figure 2 GO analyses of host proteins in the PPI networks

A. Enriched GO terms in the categories of molecular function, biological process, and cellular component are found in both shared and virus-specific PPI networks. The folds of enrichment are color-coded by *P* value. As examples, interactions of six non-structural ZIKV proteins (NS2B, NS3, NS4A, NS4A + 2K, 2K + NS4B, and NS5) with proteasome complex (**B**) and interactions of eight non-structural ZIKV proteins (NS2A, NS2B, NS3, NS4A, NS4A + 2K, 2K + NS4B, SN4B, and NS5) with spliceosome complex (**C**) were shown respectively. Here, only the subunits capable of binding with ZIKV proteins were included. Circles with bright blue outlines indicate previously reported virus binding proteins. **D.** Co-IP of overexpressed FLAG-tagged ZIKV proteins (NS3 and NS5) and V5-tagged human proteasome subunits (PSMA1, PSMA3, and PSMB4) in HEK293FT cells. IP assays were performed with anti-FLAG mAb magnetic beads and eluted fractions were analyzed by Western blot using mouse anti-V5 antibodies. Mouse IgG magnetic beads were used as a negative control to evaluate any non-specific binding on the beads. Inputs correspond to 2% of total lysate incubating with anti-FLAG mAb magnetic beads.

collection of 2816 approved drugs, and 1920 bioactive compounds [39], were screened for antiviral activity against ZIKV infection of HEK293 cells. ZIKV infection was quantified by ZIKV-NS1 antibody-based Time-Resolved Fluorescence Resonance Energy Transfer (ZIKV-NS1 TR-FRET) detection [40]. The ZIKV-NS1 TR-FRET assay measures the total amount of intra- and extracellular NS1 protein levels in infected cell culture, which was used as an indicator for ZIKV replication levels in cells (**Figure 4**A). Of the 6016 compounds, 256 were identified as preliminary hits and selected for secondary validation by the ZIKV-NS1 TR-FRET assay and cytotoxicity evaluation in the same cells (Figure 4A, Figure S3).

Figure 3   Critical host proteins for ZIKV replication

A. STRING analysis of genes that significantly affected ZIKV replication in RNAi screening. **B.** Percentage of genes with over 30% reduction of NS1 levels by siRNA-knockdown among all genes in a specific category. The "All" group indicates the collection of 10,415 siRNA-targeted druggable genes; the "ZIKV−host PPI" group indicates the 327 genes whose protein products were found to interact with ZIKV proteins in the PPI dataset. Note the high success rate (20 out of 47 members) in the category of "Proteasome complex."

Viral inhibition was confirmed for 217 of the preliminary hits, and 134 compounds exhibited greater than four-fold selectivity of ZIKV-NS1 inhibition over compound cytotoxicity (Table S5), which included the 24 compounds previously reported [41].

Based on the reported mechanisms of action (https://tripod. nih.gov/npc/), ZIKV inhibition exhibited by 92 of 134 effective compounds was mainly mediated by 12 biological categories [39]: proteasome inhibitors, antibacterials/antifungals, CDK inhibitors, PI3K inhibitors, Chk1 inhibitors, antiprotozoal

agents, DNA topoisomerase-I inhibitors, kinase inhibitors, inosine 5′-monophosphate dehydrogenase inhibitors, mTOR inhibitors, tubulin inhibitors, and anticancer agents (Figure 4B). Then, a ZIKV virus titer assay was performed to further confirm the anti-ZIKV activity of these compounds. Among these compounds, the antiviral activity of emetine was confirmed in the mouse models of ZIKV infection [42], which validated our compound screening approach.

Integrative analysis of the omics data

We compared data deposited in Drugbank [43], Therapeutic Target Database (TTD) [44], and STITCH 5.0 [45] and identified 1065 human proteins as targets of the 134 effective anti-ZIKV compounds from our screen. Of the 1065 protein targets, 45 were found to interact with ZIKV proteins in our PPI analysis (Figure 5A). STRING analysis revealed that the majority of these proteins (80.0%, 36/45) were highly connected via functional associations, such as physical interactions, co-expression, tissue specificity, and functional similarity [46]. Indeed, 46 connections were found among 45 proteins, compared to only 18 expected connections (PPI enrichment P value = 1.3E−8). GO analysis of these proteins revealed significant enrichment in proteasome, vesicle, and in the regulation of cell death (Figure 5A; Table S6).

Among the 6016 tested compounds, 3671 have known targets. Of these 3671 compounds, 98 (2.67%) showed selective inhibition against ZIKV infection. For the 766 drugs that are

known to target proteins in our PPI analysis, 29 (3.79%) were effective, demonstrating a 1.42-fold enrichment. Individual pathways and complexes also showed enrichment for identified effective drugs, except for peroxisome and oxidation–reduction process (Figure 5B).

Proteasome inhibitors suppress ZIKV and DENV replication

The integration of the three orthogonal datasets presented strong evidence that the same conserved cellular machineries play an important role in ZIKV and DENV replication. The proteasome complex stood out for several reasons. First, the PPI network analysis revealed that six ZIKV and six DENV proteins interacted with eight and seven proteasome subunits, respectively, most of which are part of the 20S core particle (Figure 6A and B). Second, individual knockdown of 20 proteasome genes resulted in substantially reduced ZIKV replication in the RNAi screen (Figure 3B). Third, the proteasome complex was the most significantly enriched pathway targeted by the 134 effective compounds identified by the chemical genetics approach to inhibit ZIKV.

To further validate our results, we selected six proteasome inhibitors (MLN-2238, carfilzomib, bortezomib, delanzomib, oprozomib, and MG-115) for further evaluation of their inhibitory activities on ZIKV and DENV in the human glioblastoma cell line SNB-19. We used a recent clinical isolate of the Puerto Rico PRVABC59 ZIKV strain for this analysis. The cultures were infected with ZIKV or DENV at a multiplic-
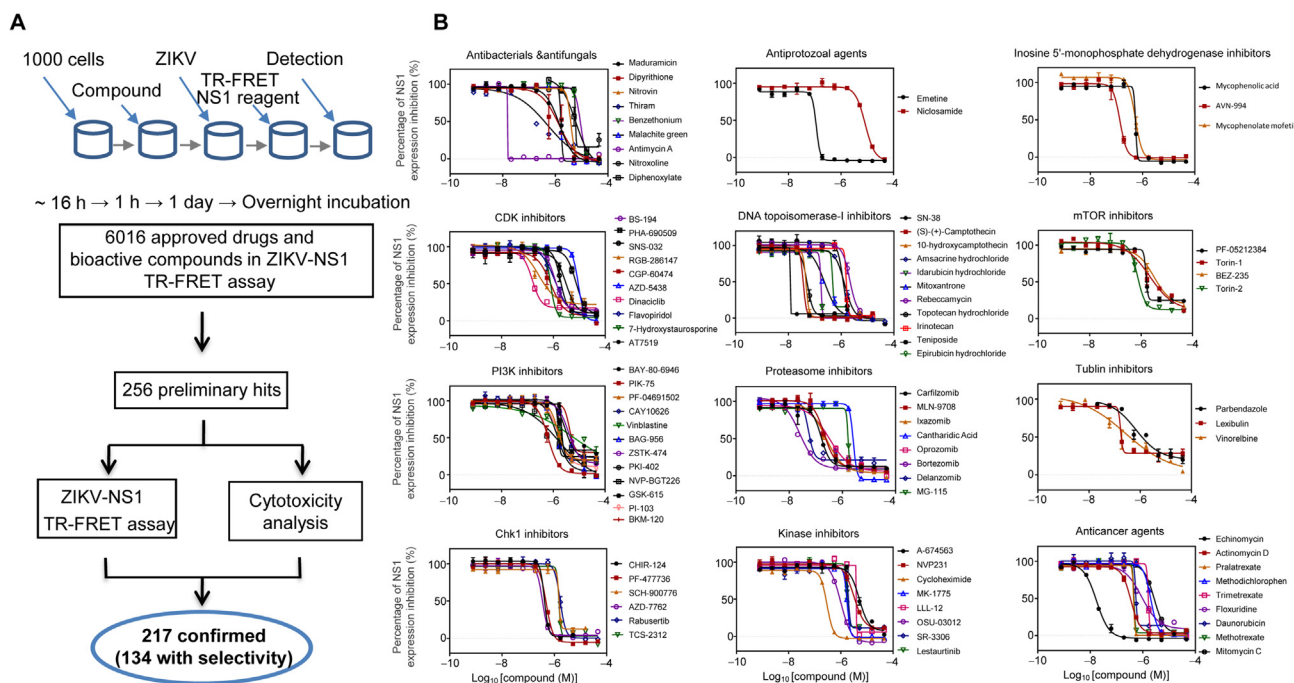

Figure 4　Small molecule inhibitors against ZIKV replication
A. Flowchart of compound screening and confirmation with the ZIKV-NS1 TR-FRET assay. Precultured cells in 1536-well plates were treated with 6016 compounds for 1 h, and then infected with virus for 1 day, followed by the ZIKV-NS1 TR-FRET assay. Of the 6016 compounds, 256 were identified as preliminary hits and selected for secondary validation by the ZIKV-NS1 TR-FRET assay and cytotoxicity evaluation with the same cells. 217 of the preliminary hits were confirmed and 134 compounds exhibited greater than four-fold selectivity of ZIKV-NS1 inhibition over compound cytotoxicity. **B.** Summary of behaviors and IC$_{50}$ values of 12 groups of potent compounds categorized based upon their reported mechanisms of action. Values represent mean ± SD (n = 3 cultures). Curves represent best fits for calculating IC$_{50}$.
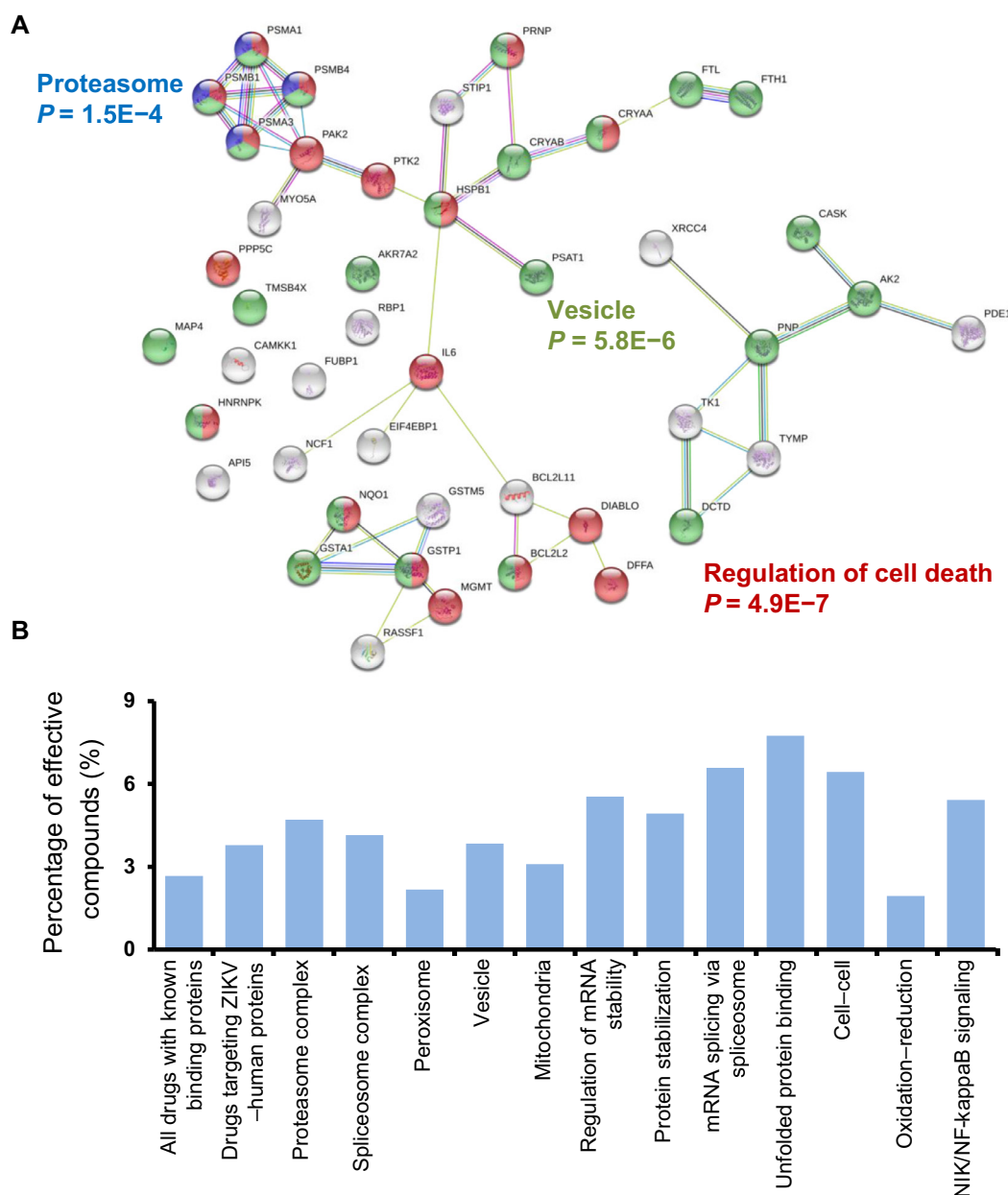
Figure 5   Integrative analysis of PPI and chemical genetics screen
A. STRING analysis of 45 anti-ZIKV drug target human proteins that were found to interact with ZIKV proteins in our PPI analysis. **B.** Functional association networks among the proteins that interact with viral proteins and are targeted by effective compounds.

ity of infection (MOI) of 1 in the presence of these compounds at a concentration of 1 μM. DMSO served as the negative control. In this assay, all of the proteasome inhibitors tested suppressed both of ZIKV and DENV envelope expression as compared to the DMSO control (Figure 6C, Figure S4A and B).

Finally, we used a colorimetric focus-forming unit (FFU) assay to determine the dose response and IC_{50} of these compounds on ZIKV production. Consistent with the intracellular antigen expression assay, all six proteasome inhibitors reduced infectious ZIKV production, with IC_{50} values for MLN-2238, carfilzomib, bortezomib, delanzomib, and oprozomib in the nanomolar range (Figure 6D and E).

Discussion

In this study, we employed three high-throughput platforms to investigate host cellular machineries that are critical for ZIKV and DENV replication. First, HuProt arrays were used to screen for direct PPIs between each ZIKV/DENV protein and 20,240 human proteins. Next, an RNAi screen targeting 10,415 druggable genes was adapted to identify the critical human genes required for ZIKV replication. Lastly, a chemical genetics approach was employed to screen 6016 bioactive compounds for their ability to inhibit ZIKV replication. We have confirmed the anti-ZIKV activities of 217 compounds, with 134 of them having a selectivity index greater than 4-fold,
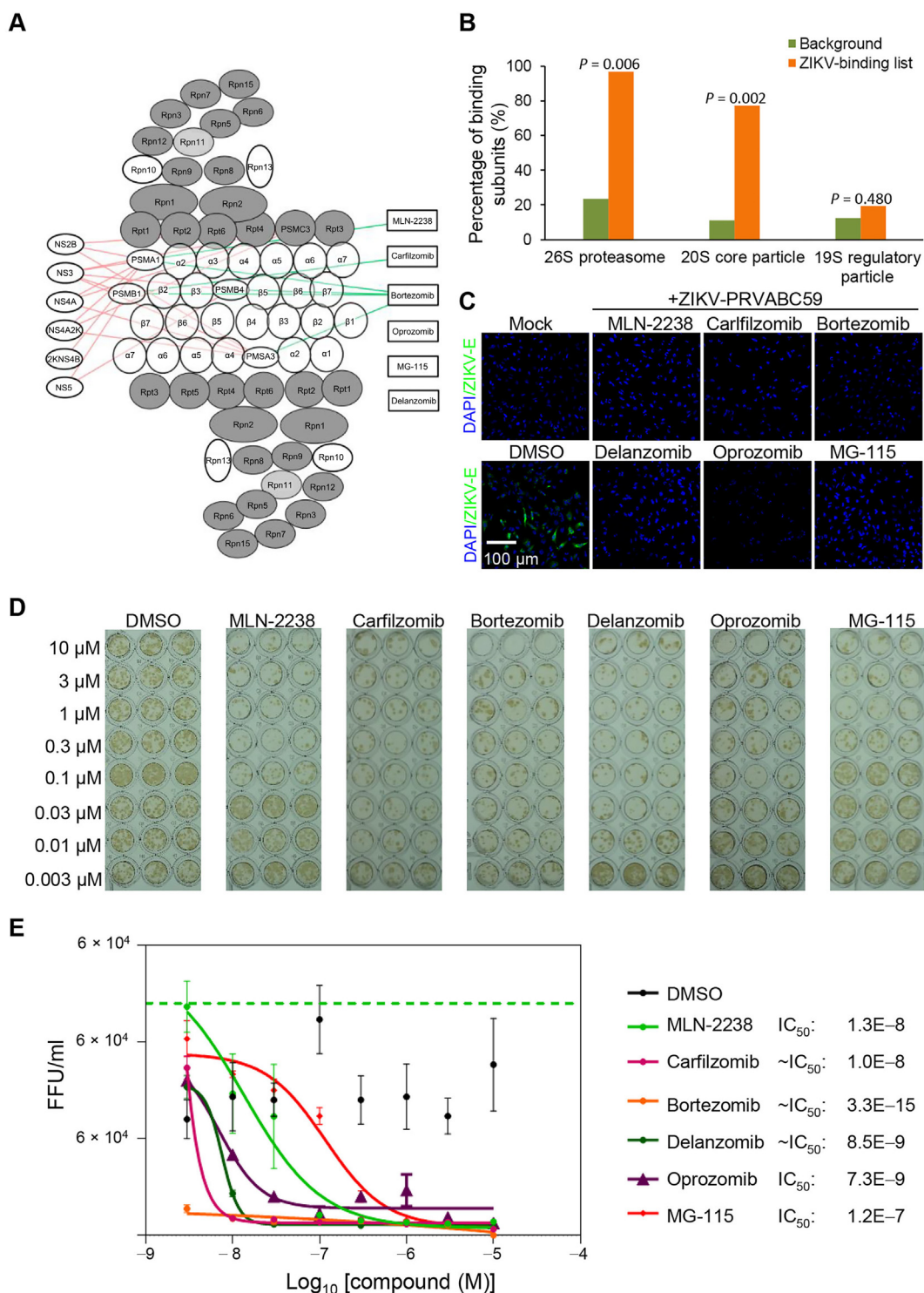
Figure 6   Experimental validation of the proteasome inhibitors

A. PPI network analysis of virus proteins and human proteasome subunits reveals that most of the interacting proteasome subunits are part of the 20S core particle. **B.** Percentage of the ZIKV-binding subunits in 26S proteasome and its two sub-complexes, the 20S core particle and the 19S regulatory particle. **C.** Inhibition of ZIKV expression in human glioblastoma cell line SNB-19 by a panel of proteasome inhibitors. The SNB-19 cells were infected by ZIKV PRVABC59 (MOI = 1) in the presence of 1 μM of each inhibitor and then incubated for 48 h before the cultures were analyzed for ZIKV-E protein expression by immunostaining. Mock indicates cells without ZIKV infection. Scale bar: 100 μm. **D.** and **E.** Sample images (D) and quantification (E) of titer assay to assess the potency of the proteasome inhibitors against infectious ZIKV production in SNB-19 cells. All data were normalized to that of 0 μM for each compound. Dose-dependent antiviral activity is presented as fluorescent focus-forming units per ml (FFU/ml) and data are represented as mean ± SD ($n = 6$). Curves represent best fits for calculating IC_{50} values (listed to the right). MOI, multiplicity of infection; ZIKV-E, ZIKV envelope.

which represents a comprehensive list of approved drugs and bioactive compounds with anti-ZIKV activity. Integration of the three independent omics datasets identified several host machineries, including the proteasome complex, the spliceosome complex, and regulation of mRNA stability. The integrated data, including PPIs, RNAi screening, and compound screening focused on ZIKV and DENV, provide useful resources for further studies to understand viral biology and disease pathogenesis and to identify new drug targets. Moreover, the systematic screening illustrated by our approach can be readily implemented to study other virus–host interactions in order to uncover the nuances of disease pathogenesis and discover novel therapeutic strategies.

Our multi-omics datasets could have many applications. As an example, we recently took advantage of the PPI dataset to understand molecular mechanisms underlying the differential pathogenic impact on host cells induced by ZIKV and DENV [27]. Consistent with the clinical phenotype that ZIKV infection, but not DENV infection, could lead to microcephaly, our functional screen showed that expression of ZIKV-NS2A, but not DENV-NS2A, leads to reduced proliferation and accelerated depletion of cortical neural stem cells in both embryonic mouse cortex *in vivo* and cultured human forebrain organoids. To understand how these two very similar proteins lead to different consequences in the same host cells, we mined the PPI dataset (Table S2) and found differential interactions of ZIKV-NS2A and DENV-NS2A with adherens junction proteins. We further validated this finding in neural stem cells with endogenous proteins [27]. This critical information generated the hypothesis that the differential impact of ZIKV-NS2A and DENV-NS2A on adherens junctions may underlie their differential impact on neural stem cell properties. We tested and confirmed this hypothesis in both *in vivo* embryonic mouse cortex and *in vitro* human brain organoid models [27]. Other viral proteins have also been implicated in the pathogenesis of virus infection; for example, ZIKV-NS4A and ZIKV-NS4B cooperatively suppressed the Akt-mTOR pathway to inhibit neurogenesis and induce autophagy in human fetal neural stem cell [47]. Additionally, we found that targeting multiple components of the same protein complexes/signaling pathways seems to be a reoccurring event in pathogen–host interactions. Using the spliceosome complex as an example (Figure 2C), host proteins API5 and HNRNPDL were found to interact with ZIKV proteins NS4A and NS5, respectively. It is an intriguing finding that the same process/complex can be targeted by a pathogen at different times. It is conceivable that such "multivalency" interactions could serve as an effective means to ensure the robust hijacking of the host cell machinery by a pathogen. For example, in one of our previous studies using *in vitro* phosphorylation assays on human protein arrays, we observed that four conserved viral protein kinases encoded by four different herpesviruses could all phosphorylate 14 components of the DNA damage response pathways, such as TIP60, RAD51, RPA1, and RPA2 [17]. In-depth *in vivo* studies confirmed that these phosphorylation events played an important role in promoting viral DNA replication in all four viruses. In another study, we observed that a secreted protein kinase ROP18, encoded by *Toxoplasma gondii*, could phosphorylate multiple components in the MAPK pathway [29]. A third example is the observation that the KSHV-encoded LANA protein could bind to all three components of the NER damage recognition/verification complex XPA–RPA (*i.e.*, XPA, RPA1, and RPA2) [48]. Therefore, our virus–host PPI database can be used to explore both conserved and unique pathogenic processes induced by ZIKV and DENV in different cellular contexts in the future.

In this study, we focused the investigation of our datasets on viral replication to identify critical cellular machineries as candidate drug targets [19]. Using high-throughput drug screening to reveal hijacked host machinery, we identified potential antiviral compounds with a higher genetic barrier for the virus to develop drug-resistance. In addition, we could potentially use these host-targeting drugs as broad-acting antivirals for closely related viruses, such as DENV and ZIKV, because of their substantially overlapping PPI networks with the host. Integrative analysis of independently identified pathways and PPI networks presents a strong case for the proteasome as a conserved, critical machinery for ZIKA and DENV replication. The proteasome complex is a part of the ubiquitin–proteasome pathway and regulates many fundamental cellular processes [49]. Emerging evidence implicates the proteasome as a critical player in viral pathogenesis by modulating the function of viral proteins to favor viral propagation and evade the host immune response [50–52]. Until now, there have been few FDA approved antiviral drugs targeting intracellular host proteins, due to the potential side effects [9]. Notably, Maraviroc, a CCR5 receptor antagonist, has been approved as an antiretroviral drug for the treatment of HIV infection, which could prevent viral entry by blocking binding of viral envelope gp120 to CCR5 [53]. Several proteasome inhibitor drugs tested in this study, including carfilzomib and bortezomib, have been approved by the FDA for the therapy of various cancers, such as breast cancer, multiple myeloma, and Hodgkin's lymphoma [54–57]. Consequently, these drugs could potentially be repurposed to further evaluate their efficacy and tolerance in a clinical setting as novel therapies for ZIKV and DENV infection.

In summary, we discovered a multitude of cellular pathways and protein complexes related to ZIKV and DENV infection by integrating three high-throughput systems biology methods, *i.e.*, ZIKA/DENV–human PPIs, a druggable gene screen, and a high-throughput chemical genetics screen. We identified the human proteasome as a conserved, critical machinery for ZIKV and DENV replication with functional confirmation by pharmacological proteasome inhibitors. We also found a comprehensive list of 134 selective ZIKV inhibitors that span over 12 cellular pathways and mechanisms. Our study provides a rich resource of multi-omics datasets for future investigation of viral pathogenesis and drug development and highlights a systematic biological approach to investigate virus–host interactions.

Materials and methods

Viral cDNA preparation

The African prototype ZIKV strain MR766 and DENV serotype 1 Hawaii strain were used to infect mosquito cells, as previously described [58]. Lysates of virus-infected mosquito cells were prepared, and 1 μg of the total RNA was used to prepare cDNA by Superscript III (Catalog No. 18080044, Thermo-Fisher Scientific, Waltham, MA) for PCR templates.

Gateway cloning and protein expression

Gateway cloning and protein expression were performed using the method as in our previous publication [59]. In short, primer sets with the *attB1* or *attB2* sequences at the 5′- and 3′-ends respectively (Table S1) were designed to amplify the full-length viral genes, which were then cloned into Gateway Entry vector pDONR221 using the Gateway recombination reaction (Catalog No. 11789021, ThermoFisher Scientific). Each initial cloning was examined by *Bsr*GI (Catalog No. R0575S, New England Biolabs, Ipswich, MA) digestion and Sanger sequencing. Then, each insert viral gene was shuttled into the yeast expression vector pEGH-A to carry out the protein expression.

Protein labeling

The quality of each ZIKV and DENV protein was determined using SDS-PAGE, followed by Coomassie staining. Proteins that passed this quality control test were then labeled directly with NHS-tethered Cy5 dye (Catalog No. GEPA15101, Sigma-Aldrich, St. Louis, MO) on glutathione beads. After quenching the dye molecules, the labeled protein was eluted and the quantity of these purified proteins was examined on SDS-PAGE gels.

Identification of virus-binding host proteins on HuProt arrays

PPI assays on the Huprot array and signal extraction of each spot were performed using the same methods described previously [27]. In short, the signal intensity (R_{ij}) of a given protein spot (i,j) was generated as foreground signal (F_{ij}) minus the corresponding background signal (B_{ij}). The averaged R_{ij} from duplicate spots was defined as the signal intensity of the protein probe (R_p). For the replicate samples, the signal profiles were quantile normalized to a merged profile. Using a similar method as described in our previous study [60], the Z-score of each binding assay with a virus protein was computed based on the distribution of R_p.

$$Z_p = \frac{R_p - \bar{N}}{SD}$$

SD and $\bar{N}$ represent the standard deviation and mean of the noise distribution on the array, respectively. A stringent cutoff ($Z \geq 15$) was used to determine the positive hits in this study. The proteins determined as positives in all assays were removed from further analysis.

Comparison to other datasets

The statistical significance of the overlap between our set of identified virus-binding human proteins and those deposited in VirusMINT and Virhostome was calculated using a hypergeometric test implemented in R [31,32]. The number of background proteins was defined as the number of unique well-annotated human proteins detected in our HuProt Array ($n = 13,816$).

Functional annotation

Database for Annotation, Visualization, and Integrated Discovery (DAVID) was used to identify the enriched functional terms (molecular function, cellular component, biological process, and KEGG pathway) for virus-binding proteins [61]. Some enriched terms (P value < 0.05) were selected and represented in a heat map by the fold change.

PPI network

Virus–human PPIs identified in this study were input into Cytoscape to construct flavivirus–host PPI networks [62]. Human PPIs were extracted and drawn from STRING 10.0 [46]. The significance of functional terms and interaction numbers were also calculated and provided by STRING.

Drug–target interaction

Drug targets were collected from three resources, Drugbank, TTD, and STITCH 5.0 [43–45]. Drugbank and TTD include known targets of experimental drugs and FDA-approved drugs. STITCH combines chemical–protein interactions from experimental chemical screens, prediction, known databases, and text mining. For chemical–protein interactions in STITCH 5.0, only those with greater than 0.7 of high combined confidence score and with experimental or database scores were chosen for analysis. Those targets not identified as positive hits on HuProt arrays were removed from this study.

Propagation of ZIKV

ZIKV stocks were generated in *Aedes albopictus* clone C6/36 cells as previously described [40]. The ZIKV PRVABC59 strain was purchased from American Type Culture Collection (ATCC; Manassas, VA). The ZIKV MR766 stock was purchased from Zeptomatrix, Buffalo, NY. Briefly, a T-75 flask of C6/36 cells (90%–95% confluency) was inoculated with 1×10^6 ZIKV virions in low volume (3 ml) for 1 h, rocking it every 15 min. After 1 h, 17 ml of media was added and C6/36 cells were maintained at 28 °C in 5% CO_2. At 7–8 days post-viral inoculation, supernatants were harvested, filtered, and stored at −80 °C. ZIKV titer was determined by an FFU assay.

Viral infection

For SNB-19 and HEK293 cell infections, cells were seeded into 12- or 96-well plates 1 day prior to viral infection. For SNB-19 cells, compounds were added 1 h before addition of ZIKV at MOI = 1. SNB-19 cells were harvested at 48 h after infection for analysis by immunofluorescence. For viral production assays, infected SNB-19 cell supernatant was harvested 24 h post infection. ZIKV and DENV titers in cell supernatants were measured by an FFU assay (FFU/ml), as previously described [40].

Co-IP and Western blot

FLAG-tagged ZIKV proteins (NS3 and NS5) and V5-tagged human proteasome subunits (PSMA1, PSMA3, and PSMB4) were overexpressed in HEK293FT cells. For Co-IP assays, HEK293FT cells were incubated in the lysis buffer (Catalog No. 9803, Cell Signaling Technology, Danvers, MA) for 30 min on ice. After sonication and centrifugation, the supernatants were subjected to IP with anti-FLAG mAb magnetic beads (Catalog No. M8823, Sigma-Aldrich) at 4 °C overnight. Then, the beads were washed six times using lysis buffer and used to perform an immunoblot assay with mouse anti-V5 antibodies (Catalog No. R960-25, ThermoFisher Scientific). Mouse IgG magnetic beads (Catalog No. 5873, Cell Signaling Technology) were used as a negative control to evaluate any non-specific binding on the beads. After incubating with Alex647 labeled Rabbit anti-mouse IgG secondary antibody (Catalog No. A-21239, ThermoFisher Scientific,) and washing, the membranes were visualized with Odyssey® CLx Imaging System.

Immunocytochemistry

SNB-19 cells were seeded onto coverslips in 12-well plates 1 day prior to infection. At 24-h post infection, cells were fixed with 4% paraformaldehyde for 15 min at roon temperature, followed by three 10-min washes in PBS at room temperature and permeabilization in PBT (PBS with 0.1% Triton X-100) for 10 min at room temperature. Cells were blocked for 1 h at room temperature in PBTG, incubated with anti-flavivirus group antigen 4G2 (1:1000; catalog No. ATCC® VR-1852™, ATCC) at 4 °C, washed three times with PBS, and incubated with goat anti-mouse-FITC (1:500; catalog No. AP127F, Sigma-Aldrich) for 1 h at room temperature, followed by three 15-min washes with PBS. Coverslips were mounted and nuclei stained using VECTASHIELD (Catalog No. H-1200, Vector Labs, Burlingame, CA).

Compound screening using the ZIKV-NS1 TR-FRET assay

The primary compound screen was performed in 1536-well plates with the ZIKV-NS1 TR-FRET assay as described previously [42]. In total, there are 6016 compounds, including the LOPAC (1280 compounds; catalog No. LO1280, Sigma-Aldrich), the NCGC pharmaceutical collection of 2816 approved drugs, and 1920 bioactive compounds [39].

For compound screening, HEK293 cells were seeded at 1000 cells/well and incubated at 37 °C with 5% CO_2 for 16 h. Then, the compounds were transferred to cells in assay plates at 23 nl/well using a pintool workstation (Catalog No. NX-TR pintool station, Wako Automation, San Diego, CA) and incubated for 1 h. ZIKV (MOI = 1) was added to the assay plates at 2 μl/well followed by a 24-h incubation. For detection of NS1 protein levels, 2.5 μl/well of TR-FRET NS1 reagent mixture was added and incubated overnight at 4 °C. The plates were measured in the TR-FRET mode in an EnVision plate reader (Catalog No. 2105-0010, PerkinElmer, Waltham, MA). The experiment for hit compound confirmation was carried out in the same assay as the primary screen except that all the compounds were diluted at a 1:3 ratio for 11 concentrations. The primary screening data and the curve

fitting were analyzed as in a previous publication [63]. For the the concentration-response curves and IC50 values of compounds, the confirmation data were analyzed using Prism software (https://www.graphpad.com/, GraphPad Software San Diego, CA).

Compound cytotoxicity assay

To eliminate the false positive compounds due to compound cytotoxicity, an ATP content assay [40] was used to measure cell viability after cells were treated with compounds in the absence of ZIKV MR766 infection. Briefly, cells were plated in 1536-well white assay plates in the same way as described above. After a 24-h incubation with compounds, 3.5 μl ATP content reagent mixture (Catalog No. 6016941, PerkinElmer) was added to each well in the assay plates and incubated for 30 min at room temperature. Luminescence signals were determined in a ViewLux plate reader (Catalog No. ViewLux™ ultraHTS microplate imager, PerkinElmer). Compounds with cytotoxicity were eliminated from hit compound list as false positive compounds.

RNAi screening

RNAi screening was conducted using the Ambion Silencer® Select Human Druggable Genome siRNA Library Version 4 as described previously [64] and the HTRF assay for NS1 antigen was performed as described above. The HTRF signal for each unique non-overlapping siRNA against the target genes was normalized to a negative control targeting siRNA. The value for each siRNA was divided by the median negative control value and multiplied by 100 to generate the negative normalized metric for each well/siRNA. The median value of negative controls in each plate was used for normalization, while the positive control was set to assess the assay performance and transfection efficiency.

Data availability

The primary screening data of all 6016 compounds and the concentration-response curves and IC50 values of compounds with confirmation data were deposited into the PubChem database (PubChem: 1347053), and are publicly accessible at https://pubchem.ncbi.nlm.nih.gov/assay/assay.cgi?aid = 1347053.

CRediT author statement

Guang Song: Methodology, Validation, Investigation, Resources, Writing - original draft, Writing - review & editing, Visualization. **Emily M. Lee:** Methodology, Validation, Investigation, Resources, Writing - original draft, Visualization. **Jianbo Pan:** Methodology, Software, Data curation, Investigation, Visualization, Writing - original draft. **Miao Xu:** Methodology, Validation, Investigation, Resources, Writing - original draft. **Hee-Sool Rho:** Investigation, Resources. **Yichen Cheng:** Investigation, Resources. **Nadia Whitt:** Investigation, Resources. **Shu Yang:** Investigation, Resources. **Jennifer Kouznetsova:** Investigation, Resources. **Carleen Klumpp-Thomas:** Investigation, Resources. **Samuel G. Michael:** Investigation,

Competing interests

The authors declare no competing interests.

Supplementary material

Supplementary data to this article can be found online at https://doi.org/10.1016/j.gpb.2020.06.016.

ORCID

0000-0002-7630-716X (Guang Song)
0000-0001-8451-978X (Emily M. Lee)
0000-0001-6014-8160 (Jianbo Pan)
0000-0001-9968-733X (Miao Xu)
0000-0002-1688-3237 (Hee-Sool Rho)
0000-0003-3127-0102 (Yichen Cheng)
0000-0002-2886-9109 (Nadia Whitt)
0000-0001-8909-1962 (Shu Yang)
0000-0003-0210-0796 (Jennifer Kouznetsova)
0000-0002-6646-6132 (Carleen Klumpp-Thomas)
0000-0002-1070-6563 (Samuel G. Michael)
0000-0002-3459-392X (Cedric Moore)
0000-0003-2985-2541 (Ki-Jun Yoon)
0000-0003-4315-6710 (Kimberly M. Christian)
0000-0002-4523-9977 (Anton Simeonov)
0000-0002-7727-9287 (Wenwei Huang)
0000-0001-7285-8469 (Menghang Xia)
0000-0001-8886-8311 (Ruili Huang)
0000-0003-4924-6493 (Madhu Lal-Nag)
0000-0002-9358-410X (Hengli Tang)
0000-0003-1034-0757 (Wei Zheng)
0000-0002-0476-3596 (Jiang Qian)
0000-0002-8720-5310 (Hongjun Song)
0000-0002-2517-6075 (Guo-li Ming)
0000-0002-8426-2889 (Heng Zhu)

References

[1] Lindenbach BD, Thiel HJ, Rice CM. Flaviviridae: the viruses and their replication. In: Knipe DM, Howley PM, editors. Fields virology. Philadelphia: Lippincott Williams and Wilkins; 2007, p. 1101–52.

[2] Bhatt S, Gething PW, Brady OJ, Messina JP, Farlow AW, Moyes CL, et al. The global distribution and burden of dengue. Nature 2013;496:504–7.

[3] Suwanmanee S, Luplertlop N. Dengue and Zika viruses: lessons learned from the similarities between these aedes mosquito-vectored arboviruses. J Microbiol 2017;55:81–9.

[4] Johansson MA, Mier-y-Teran-Romero L, Reefhuis J, Gilboa SM, Hills SL. Zika and the risk of microcephaly. N Engl J Med 2016;375:1–4.

[5] Sessions OM, Barrows NJ, Souza-Neto JA, Robinson TJ, Hershey CL, Rodgers MA, et al. Discovery of insect and human dengue virus host factors. Nature 2009;458:1047–50.

[6] Khadka S, Vangeloff AD, Zhang C, Siddavatam P, Heaton NS, Wang L, et al. A physical interaction network of dengue virus and human proteins. Mol Cell Proteomics 2011;10:M111.

[7] Durmuş S, Ülgen KÖ. Comparative interactomics for virus–human protein–protein interactions: DNA viruses versus RNA viruses. FEBS Open Bio 2017;7:96–107.

[8] Jean Beltran PM, Federspiel JD, Sheng X, Cristea IM. Proteomics and integrative omic approaches for understanding host–pathogen interactions and infectious diseases. Mol Syst Biol 2017;13:922.

[9] de Chassey B, Meyniel-Schicklin L, Vonderscher J, Andre P, Lotteau V. Virus-host interactomics: new insights and opportunities for antiviral drug discovery. Genome Med 2014;6:115.

[10] Brito AF, Pinney JW. Protein–protein interactions in virus–host systems. Front Microbiol 2017;8:1557.

[11] Calderone A, Licata L, Cesareni G. VirusMentha: a new resource for virus–host protein interactions. Nucleic Acids Res 2015;43: D588–92.

[12] Karlas A, Machuy N, Shin Y, Pleissner KP, Artarini A, Heuer D, et al. Genome-wide RNAi screen identifies human host factors crucial for influenza virus replication. Nature 2010;463:818–22.

[13] Konig R, Stertz S, Zhou Y, Inoue A, Hoffmann HH, Bhattacharyya S, et al. Human host factors required for influenza virus replication. Nature 2010;463:813–7.

[14] Shapira SD, Gat-Viks I, Shum BO, Dricot A, de Grace MM, Wu L, et al. A physical and regulatory map of host-influenza interactions reveals pathways in H1N1 infection. Cell 2009;139:1255–67.

[15] Uetz P, Dong YA, Zeretzke C, Atzler C, Baiker A, Berger B, et al. Herpesviral protein networks and their interaction with the human proteome. Science 2006;311:239–42.

[16] Woodard C, Liao G, Goodwin CR, Hu J, Xie Z, dos Reis TF, et al. A screen for extracellular signal-regulated kinase-primed glycogen synthase kinase 3 substrates identifies the p53 inhibitor iASPP. J Virol 2015;89:9232–41.

[17] Li R, Zhu J, Xie Z, Liao G, Liu J, Chen MR, et al. Conserved herpesvirus kinases target the DNA damage response pathway

and TIP60 histone acetyltransferase to promote virus replication. Cell Host Microbe 2011;10:390–400.

[18] Woodard C, Shamay M, Liao G, Zhu J, Ng AN, Li R, et al. Phosphorylation of the chromatin binding domain of KSHV LANA. PLoS Pathog 2012;8:e1002972.

[19] Watanabe T, Kawakami E, Shoemaker JE, Lopes TJ, Matsuoka Y, Tomita Y, et al. Influenza virus-host interactome screen as a platform for antiviral drug development. Cell Host Microbe 2014;16:795–805.

[20] Jäger S, Cimermancic P, Gulbahce N, Johnson JR, McGovern KE, Clarke SC, et al. Global landscape of HIV-human protein complexes. Nature 2012;481:365–70.

[21] Zhu J, Liao G, Shan L, Zhang J, Chen MR, Hayward GS, et al. Protein array identification of substrates of the Epstein-Barr virus protein kinase BGLF4. J Virol 2009;83:5219–31.

[22] Belshaw R, Gardner A, Rambaut A, Pybus OG. Pacing a small cage: mutation and RNA viruses. Trends Ecol Evol 2008;23:188–93.

[23] Sanjuán R, Domingo-Calap P. Mechanisms of viral mutation. Cell Mol Life Sci 2016;73:4433–48.

[24] Boldescu V, Behnam MAM, Vasilakis N, Klein CD. Broad-spectrum agents for flaviviral infections: dengue, Zika and beyond. Nat Rev Drug Discov 2017;16:565–86.

[25] Savidis G, McDougall WM, Meraner P, Perreira JM, Portmann JM, Trincucci G, et al. Identification of Zika virus and dengue virus dependency factors using functional genomics. Cell Rep 2016;16:232–46.

[26] Ma H, Dang Y, Wu Y, Jia G, Anaya E, Zhang J, et al. A CRISPR-based screen identifies genes essential for West-Nile-virus-induced cell death. Cell Rep 2015;12:673–83.

[27] Yoon KJ, Song G, Qian X, Pan J, Xu D, Rho HS, et al. Zika-virus-encoded NS2A disrupts mammalian cortical neurogenesis by degrading adherens junction proteins. Cell Stem Cell 2017;21:349–358.e6.

[28] Ming Gl, Tang H, Song H. Advances in Zika virus research: stem cell models, challenges, and opportunities. Cell Stem Cell 2016;19:690–702.

[29] Yang Z, Hou Y, Hao T, Rho HS, Wan J, Luan Y, et al. A human proteome array approach to identifying key host proteins targeted by *Toxoplasma* kinase ROP18. Mol Cell Proteomics 2017;16:469–84.

[30] Hu S, Xie Z, Onishi A, Yu X, Jiang L, Lin J, et al. Profiling the human protein-DNA interactome reveals ERK2 as a transcriptional repressor of interferon signaling. Cell 2009;139:610–22.

[31] Chatr-aryamontri A, Ceol A, Peluso D, Nardozza A, Panni S, Sacco F, et al. VirusMINT: a viral protein interaction database. Nucleic Acids Res 2009;37:D669–73.

[32] Rozenblatt-Rosen O, Deo RC, Padi M, Adelmant G, Calderwood MA, Rolland T, et al. Interpreting cancer genomes using systematic host network perturbations by tumour virus proteins. Nature 2012;487:491–5.

[33] Coyaud E, Ranadheera C, Cheng D, Gonçalves J, Dyakov BJA, Laurent EMN, et al. Global interactomics uncovers extensive organellar targeting by Zika virus. Mol Cell Proteomics 2018;17:2242–55.

[34] De Maio FA, Risso G, Iglesias NG, Shah P, Pozzi B, Gebhard LG, et al. The dengue virus NS5 protein intrudes in the cellular spliceosome and modulates splicing. PLoS Pathog 2016;12:e1005841.

[35] Tahiliani M, Koh KP, Shen Y, Pastor WA, Bandukwala H, Brudno Y, et al. Conversion of 5-methylcytosine to 5-hydroxymethylcytosine in mammalian DNA by MLL partner TET1. Science 2009;324:930–5.

[36] Tai AW, Benita Y, Peng LF, Kim SS, Sakamoto N, Xavier RJ, et al. A functional genomic screen identifies cellular cofactors of hepatitis C virus replication. Cell Host Microbe 2009;5:298–307.

[37] Wu KX, Phuektes P, Kumar P, Goh GYL, Moreau D, Chow VTK, et al. Human genome-wide RNAi screen reveals host factors required for enterovirus 71 replication. Nat Commun 2016;7:13150.

[38] Marceau CD, Puschnik AS, Majzoub K, Ooi YS, Brewer SM, Fuchs G, et al. Genetic dissection of flaviviridae host factors through genome-scale CRISPR screens. Nature 2016;535:159–63.

[39] Huang R, Southall N, Wang Y, Yasgar A, Shinn P, Jadhav A, et al. The NCGC pharmaceutical collection: a comprehensive resource of clinically approved drugs enabling repurposing and chemical genomics. Sci Transl Med 2011;3:80ps16.

[40] Xu M, Lee EM, Wen Z, Cheng Y, Huang WK, Qian X, et al. Identification of small-molecule inhibitors of Zika virus infection and induced neural cell death via a drug repurposing screen. Nat Med 2016;22:1101–7.

[41] Barrows NJ, Campos RK, Powell ST, Prasanth KR, Schott-Lerner G, Soto-Acosta R, et al. A screen of FDA-approved drugs for inhibitors of Zika virus infection. Cell Host Microbe 2016;20:259–70.

[42] Yang S, Xu M, Lee EM, Gorshkov K, Shiryaev SA, He SH, et al. Emetine inhibits Zika and Ebola virus infections through two molecular mechanisms: inhibiting viral replication and decreasing viral entry. Cell Discov 2018;4:31.

[43] Law V, Knox C, Djoumbou Y, Jewison T, Guo AC, Liu Y, et al. DrugBank 4.0: shedding new light on drug metabolism. Nucleic Acids Res 2014;42:D1091–7.

[44] Yang H, Qin C, Li YH, Tao L, Zhou J, Yu CY, et al. Therapeutic target database update 2016: enriched resource for bench to clinical drug target and targeted pathway information. Nucleic Acids Res 2016;44:D1069–74.

[45] Szklarczyk D, Santos A, von Mering C, Jensen LJ, Bork P, Kuhn M. STITCH 5: augmenting protein–chemical interaction networks with tissue and affinity data. Nucleic Acids Res 2016;44:D380–4.

[46] Szklarczyk D, Franceschini A, Wyder S, Forslund K, Heller D, Huerta-Cepas J, et al. STRING v10: protein–protein interaction networks, integrated over the tree of life. Nucleic Acids Res 2015;43:D447–52.

[47] Liang Q, Luo Z, Zeng J, Chen W, Foo SS, Lee SA, et al. Zika virus NS4A and NS4B proteins deregulate Akt-mTOR signaling in human fetal neural stem cells to inhibit neurogenesis and induce autophagy. Cell Stem Cell 2016;19:663–71.

[48] Shamay M, Liu J, Li R, Liao G, Shen L, Greenway M, et al. A protein array screen for Kaposi's sarcoma-associated herpesvirus LANA interactors links LANA to TIP60, PP2A activity, and telomere shortening. J Virol 2012;86:5179–91.

[49] Chowdhury M, Enenkel C. Intracellular dynamics of the ubiquitin-proteasome-system. F1000Res 2015;4:367.

[50] Zhu J, Davoli T, Perriera JM, Chin CR, Gaiha GD, John SP, et al. Comprehensive identification of host modulators of HIV-1 replication using multiple orthologous RNAi reagents. Cell Rep 2014;9:752–66.

[51] Choi AG, Wong J, Marchant D, Luo H. The ubiquitin-proteasome system in positive-strand RNA virus infection. Rev Med Virol 2013;23:85–96.

[52] Luo H. Interplay between the virus and the ubiquitin–proteasome system: molecular mechanism of viral pathogenesis. Curr Opin Virol 2016;17:1–10.

[53] Dorr P, Westby M, Dobbs S, Griffin P, Irvine B, Macartney M, et al. Maraviroc (UK-427,857), a potent, orally bioavailable, and selective small-molecule inhibitor of chemokine receptor CCR5 with broad-spectrum anti-human immunodeficiency virus type 1 activity. Antimicrob Agents Chemother 2005;49:4721–32.

[54] Avet-Loiseau H, Fonseca R, Siegel D, Dimopoulos MA, Spicka I, Masszi T, et al. Carfilzomib significantly improves the progression-free survival of high-risk patients in multiple myeloma. Blood 2016;128:1174–80.

[55] Siegel DS, Dimopoulos MA, Ludwig H, Facon T, Goldschmidt H, Jakubowiak A, et al. Improvement in overall survival with carfilzomib, ienalidomide, and dexamethasone in patients with

relapsed or refractory multiple myeloma. J Clin Oncol 2018;36:728–34.

[56] Eichenauer DA, Plütschow A, Kreissl S, Sökler M, Hellmuth JC, Meissner J, et al. Incorporation of brentuximab vedotin into first-line treatment of advanced classical Hodgkin's lymphoma: final analysis of a phase 2 randomised trial by the German Hodgkin study group. Lancet Oncol 2017;18:1680–7.

[57] Mohan M, Matin A, Davies FE. Update on the optimal use of bortezomib in the treatment of multiple myeloma. Cancer Manag Res 2017;9:51–63.

[58] Zhang F, Hammack C, Ogden SC, Cheng Y, Lee EM, Wen Z, et al. Molecular signatures associated with ZIKV exposure in human cortical neural progenitors. Nucleic Acids Res 2016;44:8610–20.

[59] Song G, Rho HS, Pan J, Ramos P, Yoon KJ, Medina FA, et al. Multiplexed biomarker panels discriminate Zika and dengue virus infection in humans. Mol Cell Proteomics 2018;17:349–56.

[60] Hu S, Wan J, Su Y, Song Q, Zeng Y, Nguyen HN, et al. DNA methylation presents distinct binding sites for human transcription factors. Elife 2013;2:e00726.

[61] Huang DW, Sherman BT, Lempicki RA. Systematic and integrative analysis of large gene lists using DAVID bioinformatics resources. Nat Protoc 2009;4:44–57.

[62] Shannon P, Markiel A, Ozier O, Baliga NS, Wang JT, Ramage D, et al. Cytoscape: a software environment for integrated models of biomolecular interaction networks. Genome Res 2003;13:2498–504.

[63] Wang Y, Jadhav A, Southal N, Huang R, Nguyen D-T. A grid algorithm for high throughput fitting of dose-response curve data. Curr Chem Genomics 2010;4:57–66.

[64] Panda D, Fernandez DJ, Lal M, Buehler E, Moss B. Triad of human cellular proteins, IRF2, FAM111A, and RFC3, restrict replication of orthopoxvirus SPI-1 host-range mutants. Proc Natl Acad Sci U S A 2017;114:3720–5.